doi:10.1017/S1431927619001065
Microsc. Microanal. 25 (Suppl 2), 2019

Electromagnetic Field Reconstructions of 4D-STEM Datasets using Ptychography and Differential Phase Contrast Imaging

Shaohong Cao[1*], Miaofang Chi[1] and Karren L. More[1]

[1.] Center for Nanophase Materials Sciences, Oak Ridge National Laboratory, Oak Ridge, TN USA.
* Corresponding author: caos@ornl.gov

The development of fast acquisition cameras allows for the collection of a series of convergent beam electron diffraction (CBED) patterns at each scanning position during conventional STEM at a speed as fast as μs/frame. Thus, a 4D-STEM dataset (2D in real space as a function of probe position and 2D diffraction pattern in each real space position) is generated while high-angle annular dark field (HAADF)-STEM images of the sample are acquired. By analyzing the 4D-STEM dataset, we can achieve more accurate structural information than conventional STEM images acquired at a lower electron dose, i.e., imaging both the heavy (conventionally seen by annular dark field – ADF) and light (conventionally seen by annular bright field – ABF) elements at atomic resolution simultaneously. Moreover, 4D-STEM dataset analysis can reveal the field information of the sample such as the electric field, magnetic field, atomic potential, and strain. There are several techniques that have been commonly used to extract information from scanning CBED patterns, such as differential phase contrast (DPC) ptychography. By calculating the center of mass (COM) of the CBED patterns, which is the derivative of the first moment, DPC generates a qualitative solution that is linear to the electromagnetic field of the sample [1-3]. Ptychography is a more complicated phase retrieval method that either employs iterative algorithms [4-6] or phases up the transfer function of the 4D-STEM dataset [7] [8] to quantify the projected potential.

Even though ptychography extracts the projected potential quantitively and DPC extracts the projected field qualitatively, both present similar information for the sample. Some investigations have compared the calculated results from ptychography and DPC. Yang et al., [9] compared the phase contrast transfer functions (PCTF) of several experimental ptychography setups and DPC directly and showed that ptychography implemented on a Matched Illumination Detector Interferometry (MIDI)-STEM setup gives the best PCTF; Pennycook et al., [8] and Yang et al., [10] compared the DPC results from a segmented detector and ptychography results from a focused beam setup from Wigner Distribution Deconvolution (WDD) or Single-Side Band (SSB) methods and showed that ptychography provides better phase contrast than DPC; in another study [11] focused probe ptychography and COM DPC results were compared using the same dataset from a monolayer material and showed that ptychography demonstrates a higher spatial resolution than DPC. While each of these investigations derived from either the calculated transfer function [9], a specific experimental setup [8] [10], or a 2D material [11], here we deliver a comprehensive comparison between ptychography with a focused and a defocused setup and COM DPC on a bulk material. Together with simulations t, we clearly show how ptychography and DPC transfer each of the frequencies of the sample in their reconstructions.

The data was collected on a JEOL NEOARM in STEM mode at an accelerating voltage of 200kV. The sample used for this experiment was bulk $SrTiO_3$ (STO). The defocused dataset was collected at ~22nm defocus plane where the probe size was ~1nm; the convergence angle was 40mrad and camera length was 0.077m. The focused dataset was collected with a convergence angle of 10 mrad and camera length of 0.258m. A 256×256 array of CBED patterns was collected over a field of view of 13.3nm for both the defocused and focused datasets using a pnCCD detector. Figure 1(left) shows the reconstructions and

corresponding Fourier transforms of ptychography and DPC from the defocused dataset; Figure 1(right) shows the reconstructions and corresponding Fourier transforms of ptychography and DPC from the focused dataset. Our investigations show that ptychography has obvious advantages of spatial resolution and enhanced contrast on data collected with a broad beam while a sufficiently narrow beam does not provide enough illumination overlap between the adjacent scanning positions in real space and ePIE failed to converge to the global minimum. The high-resolution, low-dose characteristics of broad beam electron ptychography show its substantial advantages for characterization of radiation-sensitive materials.

References:
[1] H Rose, Ultramicroscopy **2** (1977), p. 251.
[2] JN Chapman et al., IEEE Transactions OB Magnetics **26** (1990), p. 1506.
[3] T Seki et al., Ultramicroscopy **182** (2017), p. 258.
[4] JM Rodenburg and HML Faulkner, Applied Physics Letters **85** (2004), p. 4795.
[5] AM Maiden and JM Rodenburg, Ultramicroscopy **109** (2009), p. 1256.
[6] P Thibault et al., Ultramicroscopy **109** (2009), p. 338.
[7] JM Rodenburg and RHT Bates, Phil. Trans. **339** (1992), p. 521.
[8] TJ Pennycook et al., Ultramicroscopy **151** (2014), p. 160.
[9] H Yang et al., Ultramicroscopy **171** (2016), p. 117.
[10] H Yang et al., Ultramicroscopy **151**, (2015), p. 232.
[11] Y Jiang et al., Nature **559** (2018), p. 343.
[12] Research sponsored by the Fuel Cell Technologies Office, Office of Energy Efficiency and Renewable Energy, U.S. Department of Energy. Microscopy conducted as part of a user project at ORNL's Center for Nanophase Materials Sciences, which is a U.S. Department of Energy Office of Science User Facility.

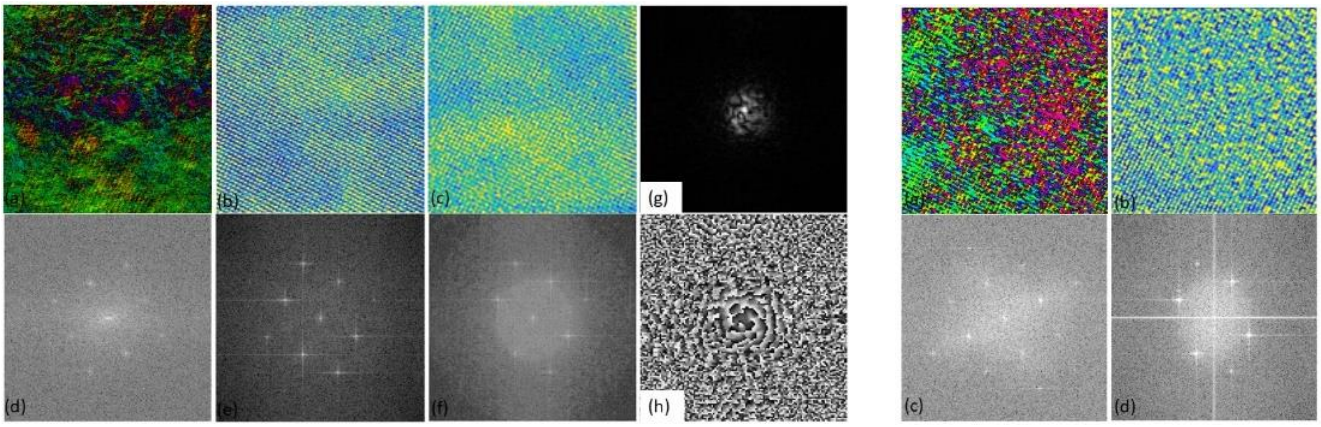

Figure 1 (left). Ptychographic and DPC reconstruction results on defocused 4D-STEM dataset. (a) DPC reconstructed field; (b) ptychographic reconstructed potential; (c) ptychographic reconstructed potential convolved with ptychographic reconstructed probe function; (d-f) corresponding Fourier transforms of (a-c); (g) and (h) modulus and phase of ptychographic reconstructed probe function, respectively.

Figure 1 (right). DPC and ptychographic reconstruction results from focused dataset. (a) DPC reconstructed field; (b) ptychographic reconstructed potential; (c) and (d) corresponding Fourier transforms of (a) and (b).

https://doi.org/10.1017/S1431927619001065 Published online by Cambridge University Press